Small-angle X-ray scattering study of the morphology of blends of poly(ε-caprolactone) and polystyrene oligomer

Shuichi Nojima, Yasunori Terashima and Tamaichi Ashida
Department of Applied Chemistry, Faculty of Engineering, Nagoya University, Furo-cho, Chikusa-ku, Nagoya 464, Japan
(Received 7 February 1985; revised 30 April 1985)

A small-angle X-ray scattering (SAXS) study was carried out to investigate the morphology of blends of poly(ε-caprolactone) (PCL) and polystyrene oligomer (PSO) when the former component was crystallized. This PCL–PSO system shows an upper critical solution temperature type of phase diagram. For blends with $\phi_{PCL} < 0.8$ (ϕ_{PCL} is the weight fraction of PCL), the scattering observed is the superposition of the intensities arising from the crystalline region (made up by alternate stacking of lamellae and thin amorphous layers) and from the inhomogeneity in the system (due to the crystalline regions and the amorphous domains). For blends with $\phi_{PCL} > 0.8$, only scattering from the crystalline region was observed. From the SAXS curve, the lamella thickness l_c, the amorphous layer thickness l_a and the linear crystallinity χ_c of the crystalline region were obtained on the basis of the Hosemann–Tsvankin model. The value of l_c was 5.5 nm independent of composition, while l_a and χ_c were 8.1 nm and 0.4 for blends with $\phi_{PCL} < 0.8$ but varied linearly with composition for blends with $\phi_{PCL} > 0.8$. These parameters were also studied by the correlation function from Vonk's model.

(Keywords: polymer blends; crystallization; phase separation; morphology; small-angle X-ray scattering)

INTRODUCTION

Morphology observed in polymer blends has been attracting much attention because it has a great influence on various properties of materials[1]. The morphology is organized mainly by two factors, liquid–liquid phase separation between components and crystallization of the components.

Recently, extensive theoretical and experimental studies on the process of liquid–liquid phase separation have been carried out[2–8] and have elucidated the mechanism of phase separation, in particular that of the early stage of spinodal decomposition. The morphology of crystallization has also been studied by many authors[9–17]. The morphological study was pioneered by Ong and Price[9] on a blend of poly(ε-caprolactone) (PCL) and poly(vinyl chloride) (PVC). The morphology of the same system was further studied by Khambatta *et al.*[10] mainly by the small-angle X-ray scattering (SAXS) technique. Similar studies were extended to blends of poly(2,6-dimethylphenylene oxide)–isotactic polystyrene[11], isotactic polystyrene–atactic polystyrene[12], poly(vinylidene fluoride)–poly(methyl methacrylate)[13], and so on. In these studies, compatible blends at a temperature above the melting points of the components were used, because phase separation followed by crystallization of one component will bring an additional complexity to the morphology. Hirata and Kotaka[18] studied by thermal and dynamical analyses the effect of lower critical solution temperature (*LCST*) behaviour on the morphology and properties of blends of poly(vinylidene fluoride) (PVF_2) and poly(methyl methacrylate). They showed that the *LCST* type of phase separation has a significant effect on the final morphology yielded by a subsequent crystallization of PVF_2.

The purpose of this study is to investigate the effect of a coexistence curve of liquid–liquid phase separation in a polymer blend on the morphology when one component is crystallized, mainly using the SAXS method. A blend of poly(ε-caprolactone) (PCL) and polystyrene oligomer (PSO) was used for which an upper critical solution temperature (*UCST*) type of phase diagram was recently reported by Watanabe *et al.*[19].

EXPERIMENTAL

Materials and sample preparation

Poly(ε-caprolactone) (PCL) supplied from Scientific Polymer Products Inc. was fractionated with benzene–methanol. The weight-average molecular weight $\bar{M}_w$ and the ratio of $\bar{M}_w$ to number-average molecular weight $\bar{M}_n$ determined by a gel permeation chromatography ($\bar{M}_w/\bar{M}_n$) were 13 700 and 1.44, respectively. Polystyrene oligomer (PSO) was supplied from Toyo Soda Co.; $\bar{M}_n$ and $\bar{M}_w/\bar{M}_n$ were stated to be 950 and 1.13, respectively.

Blends of various compositions were prepared. First, appropriate amounts of PCL and PSO were dissolved in a common solvent, benzene, at a total concentration less than 15 wt%. Then the solution was cast on a glass plate and the solvent was evaporated at 80°C for 40 h. The blends were kept at a temperature above the melting point of PCL ($T_m = 60$°C) to prevent crystallization of PCL before use.

0032-3861/86/071007-07$03.00

Cloud point

The cloud point was determined by measuring the change in intensity of He–Ne laser light transmitted through 1 mm thickness of the blend[20]. The temperature $T_p(R)$ at which the blend began to get turbid when cooled at a rate R was measured for various R ranging from 0.1 to 1.0°C min^{-1}. The cloud point temperature T_p was determined by extrapolating to $R=0$.

Differential scanning calorimetry

D.s.c. measurement was carried out to obtain the crystallinity of the blend and the melting temperature of PCL in the blend. The blends, first annealed at 120°C for 3 h and then crystallized at 26.5°C for 20 h, were heated at a rate of 10°C min^{-1}.

Small-angle X-ray scattering

SAXS measurement was carried out using an Anton Paar small-angle camera equipped with a Kratky collimation system and a step scanning scintillation counter. The radiation used was CuKα ($\lambda=1.542$ Å) monochromatized by a Ni filter, a pulse-height analyser being used. The widths of the entrance and counter slits were 100 μm and 75 μm, respectively, and the distance between the sample and the plane of registration was 21.0 cm.

The correction for finite slit width and length was carried out by Glatter's method[22] to obtain the desmeared SAXS intensity I'_{des}. The background intensity I_{back}, which represents the deviation from Porod's law, was estimated by the relation[21]

$$I'_{des}(s)=As^{-4}+I_{back} \tag{1}$$

in an intermediate range of s, where s is $(2\sin\theta)/\lambda, 2\theta$ is the scattering angle, and A is a constant. Then the intensity corrected for background, I_{des}, was obtained by subtracting I_{back} from I'_{des}. After extrapolating the corrected intensity to smaller and wider angles by Guinier's and Porod's laws, respectively, the one-dimensional correlation function $\gamma(x)$ was obtained by the relation

$$\gamma(x)=\frac{\int_0^\infty s^2 I_{des}\cos(2\pi xs)\,ds}{\int_0^\infty s^2 I_{des}\,ds} \tag{2}$$

The crystallization conditions of the blends used for the SAXS measurement are shown in *Table 1*. All samples were heated at above 100°C for 3–5 h to yield a homogeneous state. Phase separation was carried out subsequently at 75°C for blends with $\phi_{PCL}<0.6$. All samples were crystallized at 26.5°C for 20 h, which is long enough to ensure the completion of the crystallization of PCL[23].

Data analysis

The alternate stacking of crystalline and amorphous layers usually observed in crystalline polymers, which will henceforth be referred to as the 'crystalline region', can be characterized by a set of parameters[24] such as lamella

Table 1 Crystallization condition of the blends used for SAXS measurement

ϕ_{PCL}	Inital state	Phase separation	Crystallization
1	100°C, 3 h	–	26.5°C, 20 h
0.952	100°C, 3 h	–	26.5°C, 20 h
0.900	100°C, 3 h	–	26.5°C, 20 h
0.850	100°C, 3 h	–	26.5°C, 20 h
0.801	100°C, 3 h	–	26.5°C, 20 h
0.746	100°C, 3 h	–	26.5°C, 20 h
0.700	100°C, 3 h	–	26.5°C, 20 h
0.600	100°C, 3 h	–	26.5°C, 20 h
0.553	130°C, 5 h	75°C, 24 h	26.5°C, 20 h
0.501	140°C, 5 h	75°C, 3 h	26.5°C, 20 h
0.452	160°C, 5 h	75°C, 24 h	26.5°C, 20 h
0.204	170°C, 5 h	–	26.5°C, 20 h

thickness l_c, amorphous layer thickness l_a, their distributions β_c and β_a, and so on. In both the SAXS intensity curve and the correlation function, these parameters are determined so that the theoretical function derived from the appropriate model reproduces the experimental results satisfactorily. In this study, the Hosemann–Tsvankin model[25] was used for the theoretical calculation of SAXS intensity curves, and the Vonk model[26] was used for the estimation of the one-dimensional correlation function.

The scattering intensity $i(s)$ for the one-dimensional model of Hosemann–Tsvankin is given by[25]

$$i(s)=\frac{1}{2\pi^2 s^2}\left\{\mathrm{Re}\left(N\frac{(1-f_c)(1-f_a)}{1-f_cf_a}\right)+\mathrm{Re}\left[f_a\left(\frac{1-f_c}{1-f_cf_a}\right)^2[1-f_cf_a)^N]\right]\right\}Z(s) \tag{3}$$

where $Z(s)$ is a transition term, N is the mean number of stacks of lamellae within a crystalline region, and f_c and f_a are the Fourier transforms of the thickness distribution functions $h_c(x)$ and $h_a(x)$ of the crystalline and amorphous layers, respectively. Functions $h_c(x)$ and $h_a(x)$ were assumed to be Gaussian, namely

$$h_c(x)=\frac{1}{\beta_c(2\pi)^{1/2}}\exp\left(-\frac{(x-l_c)^2}{2\beta_c^2}\right) \tag{4}$$

$$h_a(x)=\frac{1}{\beta_a(2\pi)^{1/2}}\exp\left(-\frac{(x-l_a)^2}{2\beta_a^2}\right) \tag{5}$$

The transition term $Z(s)$ introduced by Tsvankin[27] is

$$Z(s)=\frac{1}{2\pi s^2 E}|1-\exp(-2\pi isE)|^2 \tag{6}$$

where E is the thickness of the transition zone between the crystalline and amorphous layers. Six parameters (l_c, l_a, β_c, β_a, N and E) were determined by fitting $i(s)$ (equation (3)) to $s^2 I_{des}$. The parameters that are more sensitive to $i(s)$, and therefore can be determined accurately, are l_c, l_a and N.

In the case of the Vonk model[26], if the same distribution functions h_c and h_a (equations (4) and (5)) as for the Hosemann–Tsvankin model are assumed, the correlation function $\gamma(x)$ is

$$\gamma(x)=\frac{\chi_c}{1-\chi_c}\left(\frac{1}{\chi_c^2}\int_0^\infty (x_c-x)h_c(x_c)\,dx_c+P_{cac}+P_{cacac}+\ldots-1\right) \tag{7}$$

where χ_x is the linear crystallinity defined as $\chi_c = l_c/(l_c + l_a)$ and the terms $P_{ca\ldots c}$ indicate convolution produces of the type $q_c h_a h_c \ldots q_c$ in which

$$q_c(x) = \int_x^\infty h_c(x_c)\,dx_c/\chi_c$$

Four parameters, l_c, l_a, β_c and β_a, were determined by the fitting procedure and from the long period L $(=l_c+l_a)$ determined from the first maximum of the experimental correlation function. The fitting was made by the Gauss–Newton method.

RESULTS AND DISCUSSION

Figure 1 shows the cloud point and melting point curves thus obtained. The cloud points could not be obtained in the vicinity of $\phi_{PCL} = 0.2$ because the decomposition of

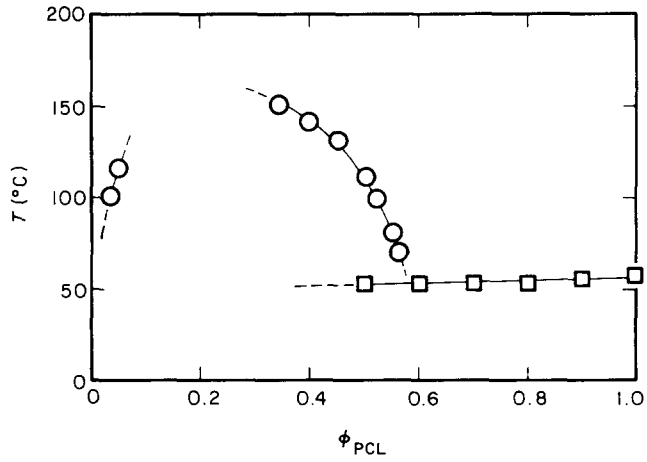

Figure 1 Cloud points (○) and melting points (□) in the PCL–PSO blend

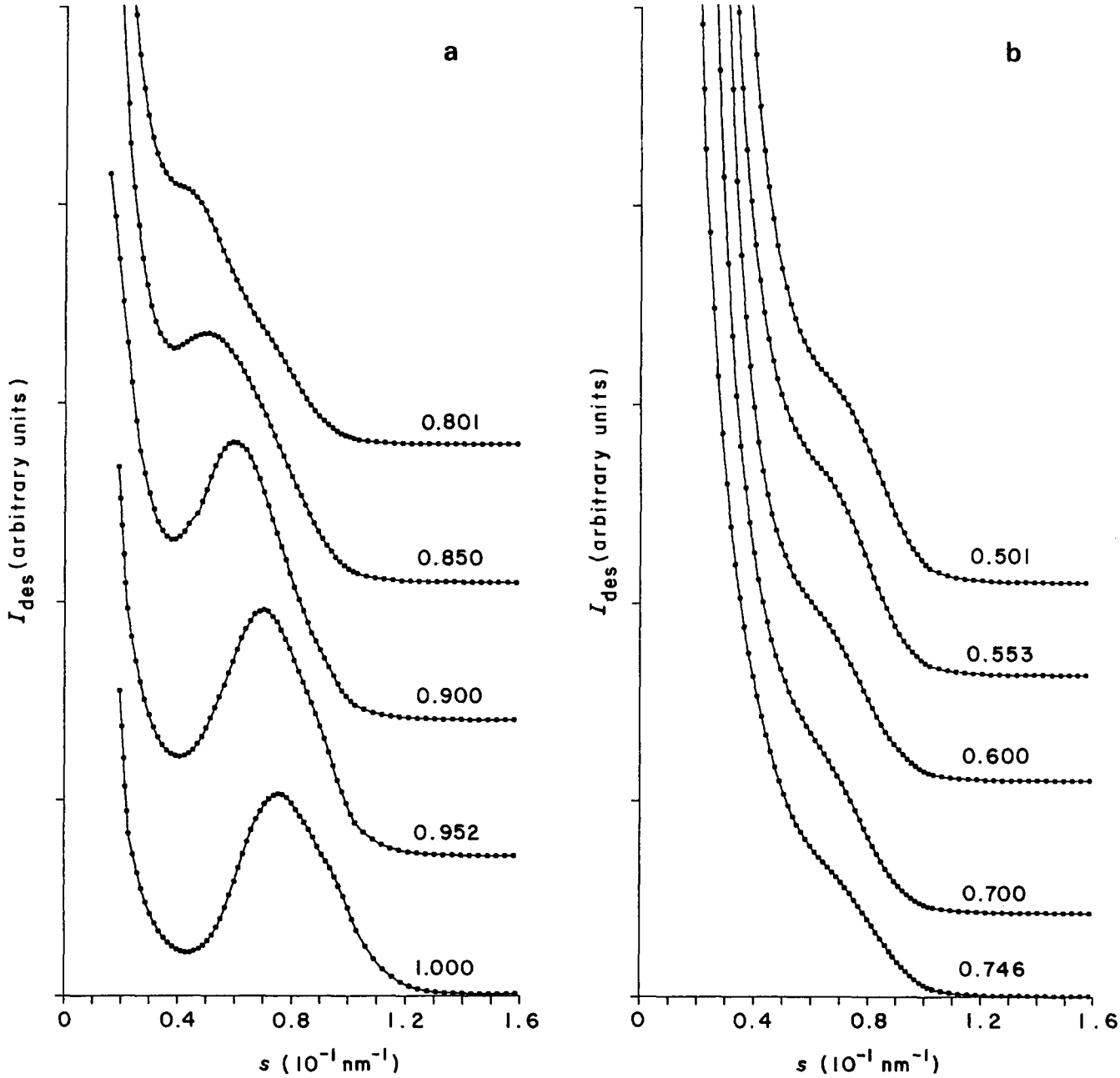

Figure 2 Experimental SAXS curves from the blends with various compositions, corrected for slit-smearing effects and the background factor. Numerals in the figure represent the weight fraction of PCL in the blend

PCL took place during annealing at a temperature above 170°C. The cloud point curve is expected to have a maximum at about $\phi_{PCL}=0.2$. The melting point curve is slightly lowered as the PCL content decreases and intersects with the cloud point curve at $\phi_{PCL}=0.6$. For compatible blends, a large depression was observed[13] and a large negative interaction parameter is derived according to the Flory–Huggins theory. A small depression in this case means that the interaction between components is not so large compared to compatible blends.

The SAXS intensity curves desmeared by Glatter's method[22], I_{des}, and those corrected by the Lorentz factor[28], s^2I_{des}, are shown in *Figures 2* and *3*, respectively. The Lorentz-corrected SAXS curves obtained from blends with $\phi_{PCL}>0.8$ (*Figure 3a*) have a peak and the corresponding wavenumber decreases with decrease of PCL content in the blend. The SAXS curves from blends with $\phi_{PCL}<0.8$ (*Figure 3b*), however, have a large scattering at smaller angles besides the peak at $s\sim7\times10^{-2}\,nm^{-1}$. The scattering at smaller angles is more marked for blends with smaller ϕ_{PCL}. The correlation functions derived for blends with $\phi_{PCL}>0.8$ are shown in *Figure 4*. The long period L obtained from the peak obviously becomes larger with decrease in PCL content in accordance with the result shown in *Figure 3a*.

The peaks at $s=(6–8)\times10^{-2}\,nm^{-1}$ (in *Figure 3*) are considered to arise from the crystalline region, which means the region of alternate stacking of lamellae and thin amorphous layers as usually observed in crystalline polymers. The scattering observed for blends with $\phi_{PCL}<0.8$ is considered to be the superposition of intensities arising from the crystalline region and from the inhomogeneity in the whole system, made up of the two-phase structure (one is the crystalline region and the other will be the amorphous domain existing outside the crystalline region in the blend). For blends with $\phi_{PCL}>0.8$, scattering from the crystalline region is mainly observed,

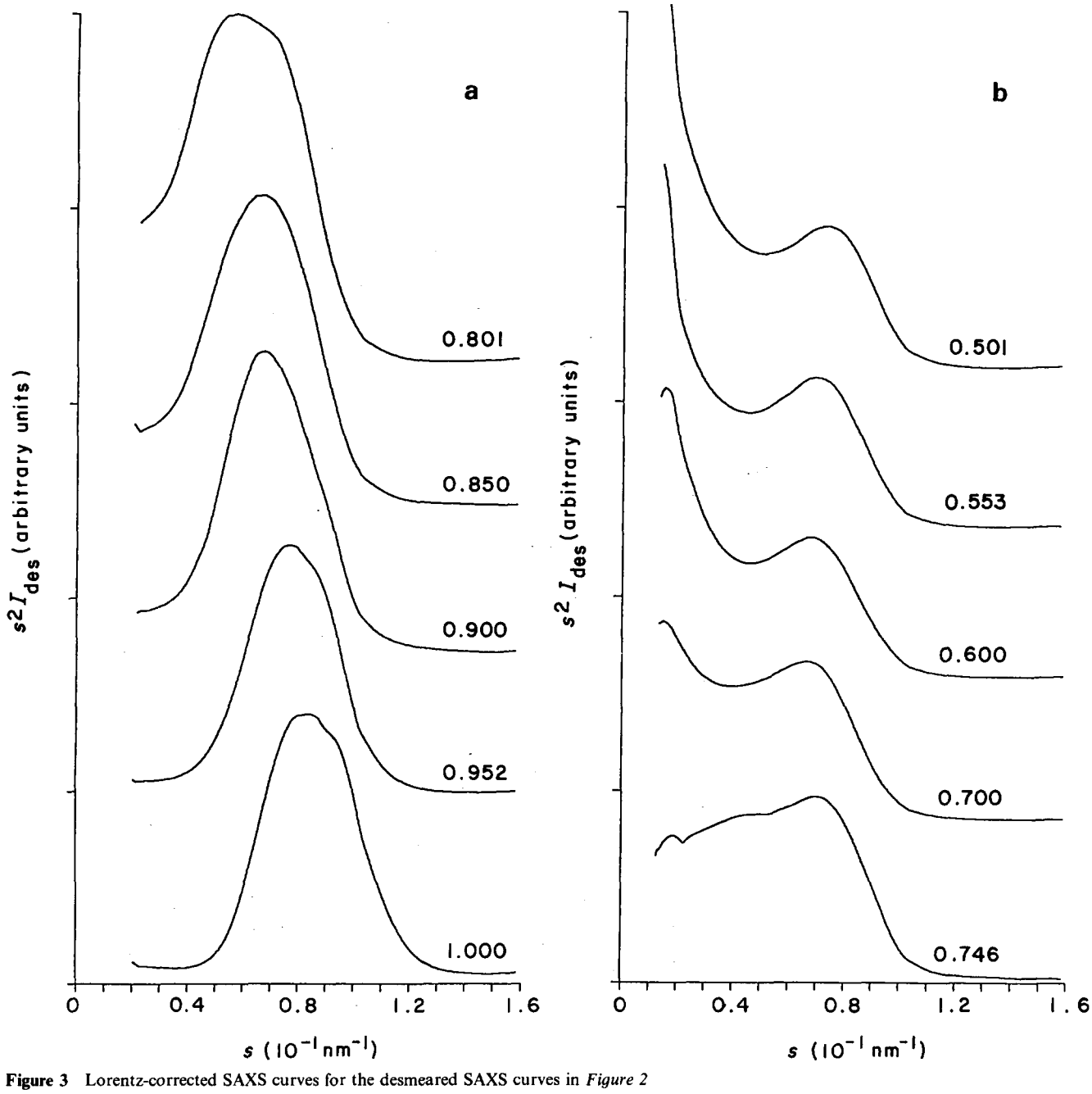

Figure 3 Lorentz-corrected SAXS curves for the desmeared SAXS curves in *Figure 2*

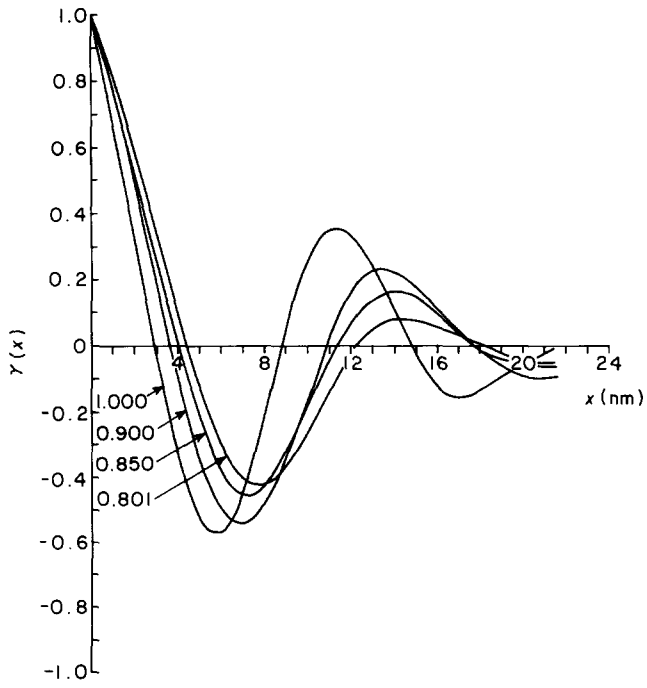

Figure 4 Experimental one-dimensional correlation function

which suggests that the system will be solely made up of crystalline regions.

The Debye–Bueche relation is generally applicable to the scattering intensity from the electron density fluctuation of inhomogeneous systems. The intensity $I(s)$ is given by[29]

$$I(s)=8\pi\langle\eta^2\rangle\xi^3/(1+4\pi^2s^2\xi^2)^2 \tag{8}$$

where $\langle\eta^2\rangle$ is the mean-square density fluctuation in the system and ξ the correlation length of the fluctuation. Equation (8) can be rewritten as

$$\frac{1}{[I(s)]^{1/2}}=\frac{4\pi^2\xi^2s^2}{(8\pi\langle\eta^2\rangle\xi^3)^{1/2}}+\frac{1}{(8\pi\langle\eta^2\rangle\xi^3)^{1/2}} \tag{9}$$

For scattering from the inhomogeneous system with correlation length ξ, $1/I_{\rm des}^{1/2}$ is linear when plotted against s^2, and ξ can be estimated from the slope and the intercept. *Figure 5* shows that plots of $1/I_{\rm des}^{1/2}$ against s^2 for blends with $\phi_{\rm PCL}<0.8$ are nearly linear at smaller s and deviate significantly from linearity at larger s. The deviation is caused by the addition of the scattering from the crystalline region. This is also understood by the fact that the linearity continues to larger s as $\phi_{\rm PCL}$ decreases. So, the linearity at smaller s represents scattering due to the inhomogeneity of the system. Thus, *Figure 5* shows that besides the crystalline region there exist amorphous domains and the scattering intensity observed in *Figures 2b* and *3b* (except that from the crystalline region) is described by the Debye–Beuche relation. The larger scattering from the inhomogeneity of the system at smaller $\phi_{\rm PCL}$ suggests that the content of amorphous domain increases as $\phi_{\rm PCL}$ decreases. The correlation length ξ derived from *Figure 5* is shown as the open circles in *Figure 6*, together with that obtained directly by fitting the sum of the theoretical intensities $i(s)$ and $s^2I(s)$ of equations (3) and (8) to the experimental intensity $s^2I_{\rm des}$ (full circles). Regardless of the bulk composition, ξ is about 11.0 nm within experimental error.

In order to obtain the parameters characterizing the crystalline region for blends with $\phi_{\rm PCL}<0.8$, the theoretical intensity must include the scattering from the inhomogeneity of the system, for which the Debye–Bueche relation (equation (8)) was used in this study. So, the measured intensity was fitted to the sum of equation (3), of which the first term corresponds to the zero-order scattering of the crystalline region, and equation (8), where ξ obtained from *Figure 5* was used and the coefficient of the intensity in equation (8) was taken as another parameter in the fitting procedure. As the PSO content increases, the scattering intensity at smaller angles becomes stronger and the residual scattering from the crystalline region becomes more ambiguous.

The fitting procedure of the theoretical intensity $i(s)$ derived from the Hosemann–Tsvankin model to the experimental SAXS curve $s^2I_{\rm des}$ for the blend with

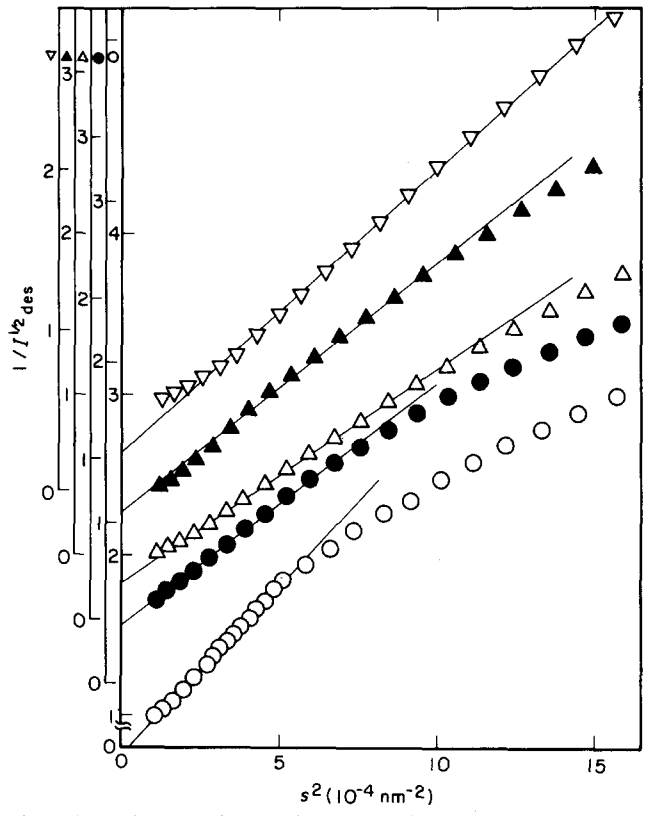

Figure 5 Debye–Bueche plot for the blends with $\phi_{\rm PCL}=0.746$ (○), 0.700 (●), 0.600 (△), 0.553 (▲) and 0.452 (▽)

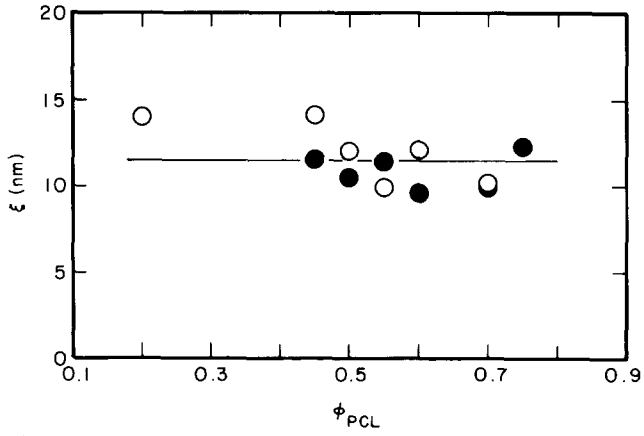

Figure 6 Correlation length ξ in the PCL–PSO blend. Open circles were obtained from Debye–Bueche plots and closed circles from the direct fitting procedure

$\phi_{PCL}=0.9$ is shown as an example in *Figure 7*, and that of the theoretical correlation function derived from Vonk's model in *Figure 8*. In *Figure 9* are shown the composition dependences of l_c, l_a and L obtained from the fitting of the Hosemann–Tsvankin model to the experimental SAXS curve. The value of l_c is about 5.5 nm regardless of composition. However, l_a and L increase with decrease in the content of PCL until ϕ_{PCL} reaches about 0.8 (denoted as ϕ^* hereafter). For blends with $\phi_{PCL}<\phi^*$, the two parameters are roughly constant, the mean values being $l_a=8.1$ nm and $L=13.6$ nm. *Figure 10* shows $\chi_c=l_c/(l_c+l_a)$

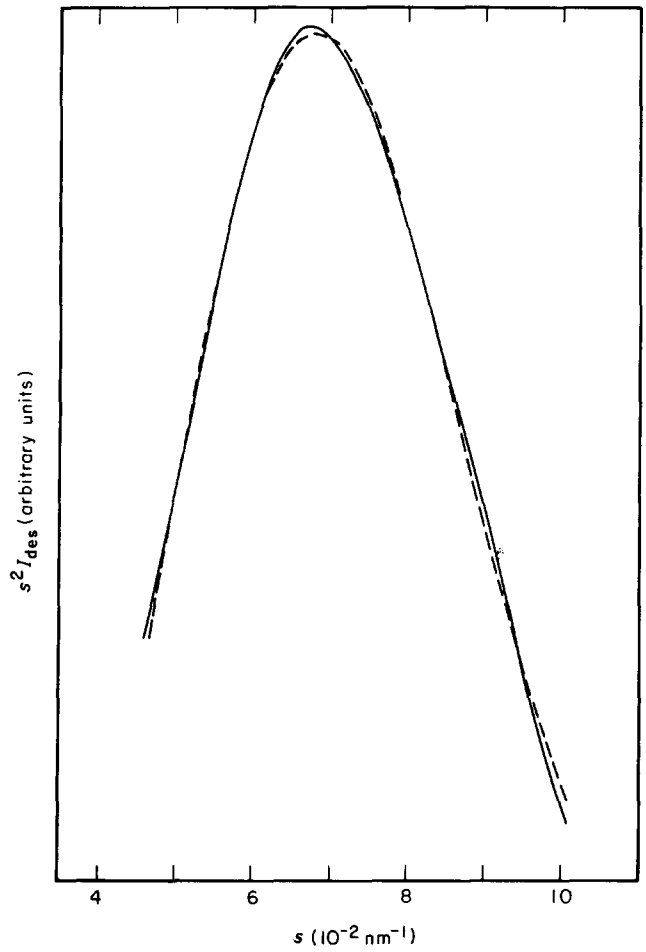

Figure 7 Experimental (———) and calculated (– – –) SAXS curves for the blend with $\phi_{PCL}=0.900$

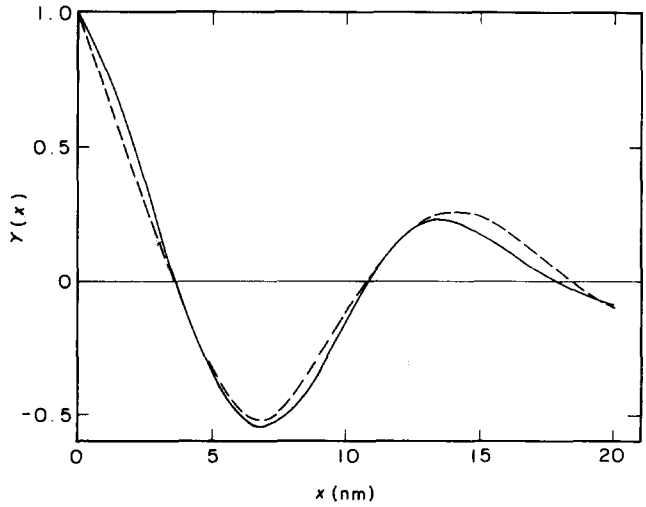

Figure 8 Experimental (———) and calculated (– – –) one-dimensional correlation functions for the blend with $\phi_{PCL}=0.900$

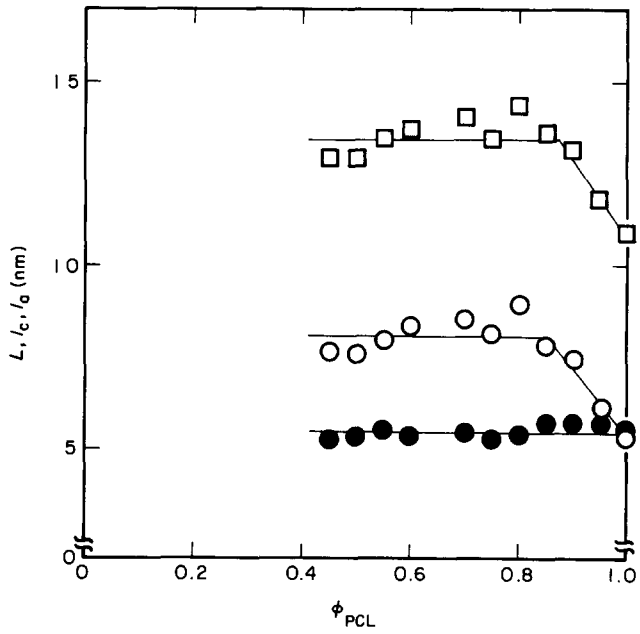

Figure 9 Composition dependence of long period, L (□), amorphous layer thickness, l_a (○) and lamella thickness, l_c (●) obtained from fitting the SAXS curve calculated from the Hosemann–Tsvankin model to that derived experimentally

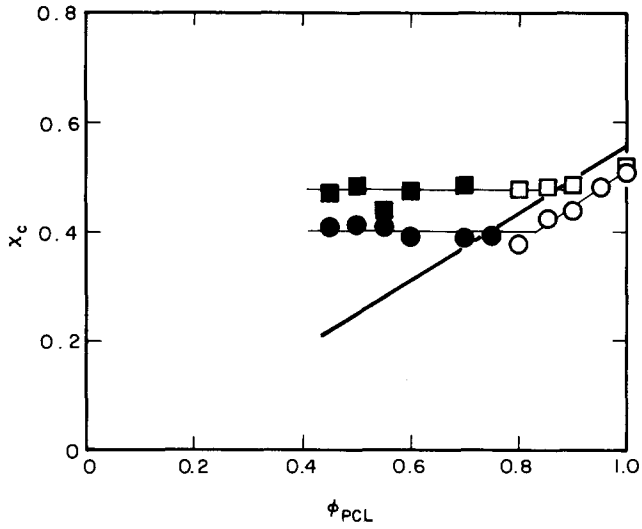

Figure 10 Composition dependence of linear crystallinity χ_c obtained from fitting the SAXS curve (●, ○) and the one-dimensional correlation function (■, □). Full symbols indicate that the scattering intensity from the amorphous region is subtracted beforehand from the measured intensity. The bold line represents the bulk crystallinity obtained from d.s.c. measurements

obtained from the Hosemann–Tsvankin and Vonk models. It is clear that the composition dependence of χ_c also changes at ϕ^*. The bold line in the figure represents the composition dependence of the bulk crystallinity derived from the d.s.c. measurement, which decreases linearly with ϕ_{PCL}.

The fact that l_a and χ_c vary for blends with $\phi^*<\phi_{PCL}\leqslant 1$ means that the amorphous component, PSO, is incorporated in the amorphous layer of PCL and this causes an increase in l_a with increase of PSO content. This situation may be similar to the case of compatible blends of poly(ε-caprolactone)–poly(vinyl chloride) studied by Khambatta *et al.*[10] and poly(2,6-dimethylphenylene oxide)–isotactic polystyrene studied by Wenig[11]. Stein *et al.*[14] explained that such a situation will be met if the distance of movement of the amorphous component

during crystallization is sufficiently shorter than the interlamellar distance. On the other hand, the morphology of the crystalline region for blends with $\phi_{PCL} < 0.8$ remains constant, that is l_c, l_a and χ_c do not change with composition in contrast with the bulk crystallinity. So, these results suggest that there are amorphous domains outside the crystalline region. This situation is similar to the morphology observed in a blend of isotactic polystyrene (i-PS) and atactic polystyrene (a-PS) studied by Warner *et al.*[12], where slow crystallization of i-PS is considered to be responsible for the organization of the morphology.

In PCL–PSO blends, the morphology formed at various compositions will also be explained by the phase separation between components. The crystallization of PCL ejects PSO to the amorphous layers between lamellae. For blends with $\phi^* < \phi_{PCL} \leqslant 1$, although the amorphous layer accommodates the excluded PSO, the PCL content of this amorphous layer still remains higher than 0.6, so that the amorphous layer is thermodynamically stable. The system is constituted from the crystalline region made up of lamellae (pure PCL) and amorphous layers (PCL + PSO), and l_a increases with decrease of ϕ_{PCL} as observed in *Figure 9*. For blends with $0.6 < \phi_{PCL} < \phi^*$, the crystallization of PCL brings about a decrease of PCL content in the amorphous layer between lamellae to $\phi_{PCL} < 0.6$. So with the crystallization of PCL the amorphous layer becomes thermodynamically unstable and undergoes phase separation if the phase diagram obtained for bulk blends (*Figure 1*) is also valid for the micro-amorphous layer. This phase separation in the amorphous layer produces two amorphous phases: one exists as the amorphous layer between lamellae with $\phi_{PCL} \sim 0.6$ and the other has the composition of nearly pure PSO. Because of large mobility due to the small molecular weight of PSO, the latter goes outside the crystalline region to form the amorphous domain. So, the composition of the amorphous layer between lamellae and therefore l_a is roughly constant regardless of ϕ_{PCL}, as observed in *Figure 9*. The composition of the amorphous domain may also be constant regardless of ϕ_{PCL}. Thus, the system is considered to be a two-phase structure made up of the crystalline region and the amorphous domain. The ratio of amorphous domain to crystalline region increases with decrease of ϕ_{PCL}. For blends with $\phi_{PCL} < 0.6$, where phase separation has taken place before the temperature reaches T_c, a heterogeneous structure composed of two phases with $\phi_{PCL} \sim 0.6$ and $\phi_{PCL} \sim 0$ prevails before the beginning of crystallization of PCL. Crystallization of PCL in the PCL-rich phase yields a PSO-rich domain (amorphous domain) also. In both cases with $0.6 < \phi_{PCL} < \phi^*$ and $\phi_{PCL} < 0.6$, nearly pure amorphous PSO domain is formed outside the crystalline region and the inhomogeneity of the system brings about large scattering at smaller s as observed in *Figures 2* and *2*.

The characteristic composition ϕ^* at which the composition dependence of l_a and χ_c changes is expected to depend on the location of the coexistence curve, because ϕ^* is affected by the composition at which phase separation begins in the amorphous layer between lamellae. This study shows that the existence of the *UCST* type of phase diagram seriously affects the morphology observed when one component crystallizes.

ACKNOWLEDGEMENTS

We wish to thank Dr Y. Muroga for his valuable advice on carrying out SAXS measurements. This work was supported by the Ministry of Education under Grant No. 58750708.

REFERENCES

1 Paul, D. R. in 'Polymer Blends', (Eds. D. R. Paul and S. Newman), Academic Press, New York, 1978, Vol. 1, Ch. 1
2 de Gennes, P. G. *J. Chem. Phys.* 1980, **72**, 4756
3 Pincus, P. *J. Chem. Phys.* 1981, **75**, 1996
4 Binder, K. *J. Chem. Phys.* 1983, **79**, 6387
5 Nojima, S., Tsutsumi, K. and Nose, T. *Polym. J.* 1982, **14**, 225
6 Gilmer, J., Goldstein, N. and Stein, R. S. *J. Polym. Sci., Polym. Phys. Edn.* 1982, **20**, 2219
7 Hashimoto, T., Kumaki, J. and Kawai, H. *Macromolecules* 1983, **16**, 641
8 Snyder, H. L., Meakin, P. and Reich, S. *Macromolecules* 1983, **16**, 757
9 Ong, C. J. and Price, F. P. *J. Polym. Sci., Polym. Symp. Edn.* 1978, **63**, 59
10 Khambatta, F. B., Warner, F., Russell, T. and Stein, R. S. *J. Polym. Sci., Polym. Phys. Edn.* 1976, **14**, 1391
11 Wenig, W., Karasz, F. E. and Macknight, W. J. *J. Appl. Phys.* 1975, **46**, 4194
12 Warner, F. P., Macknight, W. J. and Stein, R. S. *J. Polym. Sci., Polym. Phys. Edn.* 1977, **15**, 2113
13 Nishi, T. and Wang, T. T. *Macromolecules* 1975, **8**, 909
14 Stein, R. S., Khambatta, F. B., Warner, F. P., Russell, T., Escala, A. and Balizer, E. *J. Polym. Sci., Polym. Symp. Edn.* 1978, **63**, 313
15 Keith, H. D. and Padden, F. J. *J. Appl. Phys.* 1964, **35**, 1270
16 Wang, T. T. and Nishi, T. *Macromolecules* 1977, **10**, 421
17 Martuscelli, E. and Demma, G. B. in 'Polymer Blends', (Eds. E. Martuscelli, R. Palumbo and M. Kryszewski), Plenum Press, New York, 1980, p. 101
18 Hirata, Y. and Kotaka, T. *Polym. J.* 1981, **13**, 272
19 Watanabe, T., Sumi, Y., Fujiwara, Y. and Nishi, T. *Polym. Prepr. Jpn.* 1983, **31**, 886
20 Nojima, S. and Nose, T. *Polym. J.* 1982, **14**, 269
21 Vonk, C. G. in 'Small Angle X-ray Scattering', (Eds. O. Glatter and O. Kratky), Academic Press, New York, 1982, p. 433
22 Glatter, O. *J. Appl. Crystallogr.* 1974, **7**, 147
23 Koleske, J. V. in 'Polymer Blends', (Eds. D. R. Paul and S. Newman), Academic Press, New York, 1978, Vol. 2, Ch. 22
24 Strobl, G. R. and Schneider, M. *J. Polym. Sci., Polym. Phys. Edn.* 1980, **18**, 1343
25 Hosemann, R. and Bagchi, S. N. 'Direct Analysis of Diffraction by Matter', North-Holland, Amsterdam, 1965, p. 408
26 Vonk, C. G. and Kortleve, G. *Kolloid-Z. Z. Polym.* 1967, **220**, 19
27 Tsvankin, D. Y. *Polym. Sci. USSR* 1964, **6**, 2304
28 Crist, B. and Morosoff, N. *J. Polym. Sci., Polym. Phys. Edn.* 1973, **11**, 1023
29 Debye, P. and Bueche, A. M. *J. Appl. Phys.* 1949, **20**, 518